

Automatic Bone Marrow White Blood Cell Classification using Morphological Granulometric Feature of Nucleus

Shraddha Shivhare, Rajesh Shrivastava

Abstract— The differential counting of white blood cell provides invaluable information to doctors for diagnosis and treatment of many diseases. manually counting of white blood cell is a tiresome, time-consuming and susceptible to error procedure due to the tedious nature of this process, an automatic system is preferable. in this automatic process, segmentation and classification of white blood cell are the most important stages. An automatic segmentation technique for microscopic bone marrow white blood cell images is proposed in this paper. The segmentation technique segments each cell image into three regions, i.e., nucleus, cytoplasm, and background. In this paper, we investigate whether information about the nucleus alone is adequate to classify white blood cells. This is important because segmentation of nucleus is much easier than the segmentation of the entire cell, especially in the bone marrow where the white blood cell density is very high. Even though the boundaries between cell classes are not well-defined and there are classification variations among experts, we achieve a promising classification performance using neural networks with fivefold cross validation in which Bayes' classifiers and artificial neural networks are applied as classifiers. The classification performances are evaluated by two evaluation measures: traditional and classwise classification rates. we compare our results with other classifiers and previously proposed nucleus-based features. The results show that the features using nucleus alone can be utilized to achieve a classification rate of 77% on the test sets. Moreover, the classification performance is better in the class wise sense when the *a priori* information is suppressed in both the classifiers.

Index Terms—Automatic white blood cell classification, granulometric moments, mathematical morphology, pattern spectrum, white blood cell differential counts.

I. INTRODUCTION

In the traditional process, doctors analyze human blood by microscope. This manual process is time consuming and susceptible to error procedure thus, an automatic system seems necessary and helpful. The automatic DBC system may require four stages: 1) acquisition, 2) detection, 3) feature extraction, and 4) classification.

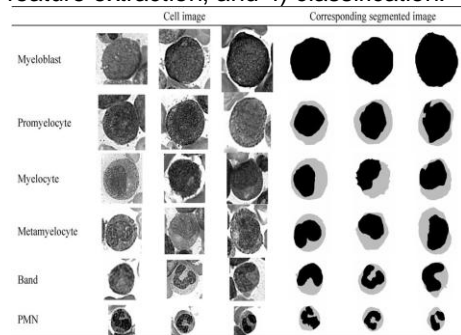


Fig. 1. Cell samples and corresponding manually segmented images in the myelocytic or granulocytic series.

In the first stage, the blood smear is magnified to a suitable scale under the microscope, and then transformed to a digital image. In the second stage, cell segmentation is used to produce a number of single-cell images. Then each single-cell image is segmented into three regions: 1) nucleus, 2) cytoplasm, and 3) background. In the third step, feature vectors of color, texture, and shape of the segmented cell and its nucleus are extracted. In the last step according to the extracted feature vectors, each WBC is labeled by a classifier. The most important stage is the cell segmentation because the accuracy of segmentation plays a crucial role in the subsequent stages. Bone marrow cells are normally diagnosed by light microscopy. Flow cytometry, which is normally used for differential blood cell counting of peripheral blood, is not suitable for bone marrow cells. This is because, in addition to its high price and complicated structure, markedly hypercellular or packed bone marrow and sclerotic bone marrow may yield too few cells for adequate analysis by flow cytometry. Data from flow cytometry should always be correlated with that from light microscopy. White blood cells in bone marrow are classified according to their maturation stages. When a white blood cell becomes older, its size, the size and shape of the nucleus, and many other characteristics change. White blood cells in the myelocytic or granulocytic series can be classified into six classes, i.e., myeloblast, promyelocyte, myelocyte, metamyelocyte, band, and polymorphonuclear (PMN) in that order from the youngest to the oldest cells. Samples of white blood cells in each of these classes are shown in Fig. 1. Three samples of each class are shown to illustrate the possible variation within each class. Due to the tediousness of manual systems, several methods have been proposed for automatic or partially automatic counting systems. Most of them, however, are for the applications in peripheral blood rather than for bone marrow. It should be noted that white blood cells in bone marrow are much denser than those in peripheral blood; therefore, segmentation of white blood

Author – Shraddha Shivhare
RGPV university, M.E. SS (IV SEM)
Shri Ram institute Of Technology
Jabalpur (M.P.),482001, India
shraddhashivhare@rediffmail.com

Co Author – Rajesh Shrivastava
RGPV University Asst Professor: CS Dept
Shri Ram institute of technology
Jabalpur (M.P.),482001, India
rajesh_5479@rediffmail.com

cells in bone marrow is a more difficult problem than segmentation in peripheral blood. Moreover, the immature cells are normally seen only in the bone marrow which, thus, makes cell classification in bone marrow a more difficult and also a complex problem. Sanei and Lee achieved classification rates of more than 95% for mature cells in normal blood, more than 85% for immature cells in the blood, but only just over 70% for immature cells in bone marrow. Most of the proposed automatic techniques follow the traditional manual process of detecting a cell, extracting its features, classifying the cell, and then updating the counts. There are three types of cells in normal human blood: red cells, leukocyte or white cells and blood platelets. Generally, red cells are simple and similar. While white cells contain nucleus and cytoplasm and there are different types of them. In our paper we are considering only the nucleus. In blood smear, number of red cells is many more than white cells. For example, an image may contain up to 100 red cells and only 1 to 3 white cells. In laboratories, haematologists analyse human blood by microscope. Their main tasks in this area are: red cell count, white cell count and blood disorder detection. It is tedious task to locate, identify and count these classes of cells. Due to the importance of these processes, an automated system seems necessary and helpful. White cells are clinically more important than red cells and many of blood disorders are related to them. Thus, accurate segmentation of these cells is very important. White blood cells count is used to determine the presence of an infection in the human body. The segmentation step is very crucial because the accuracy of the subsequent feature extraction and classification depends on the correct segmentation of white blood cells. It is also a difficult and challenging problem due to the complex nature of the cells and uncertainty in the microscopic image. Therefore, this step is the most important challenge in many literatures and improvement of cell segmentation has been the most common effort in many research works. Most of the proposed automatic techniques follow the traditional manual process of detecting a cell, extracting its features, classifying the cell, and then updating the counts. Our previous research concentrated on the counting of white blood cells specifically in bone marrow. We developed the mixing theories of mathematical morphology, and applied them to the counting problem without classification. We also developed a new training algorithm for neural networks in order to count the number of different cell classes without classification. In this paper, we propose a method for the classification of white blood cells using only their nucleus information. This idea is very useful in practice because one of the difficulties in the differential counting in bone marrow is how to deal with the cells that touch each other. This problem occurs frequently in cells of the bone marrow because there the white blood are very dense. If the cell classification is based only on the information about the nucleus, then we do not need to segment the entire cell, and only nucleus segmentation is adequate. Although many techniques have been applied to cell segmentation, this problem is not solved, especially in touching cells. To decouple the effects of segmentation errors, we extract features from manually segmented nucleus of a white blood cell based on morphological granulometries. We apply Bayes classifiers and artificial neural networks to the

problem of white blood cell classification of single-cell images and compare their results to those obtained by an expert. We also compare the results to other classifiers and other previously proposed features. In this paper we also propose an algorithm that keeps the original shape of the blood cell and uses information of this shape to split the overlapped regions by drawing a conical curve.

II METHODOLOGY

In this research, we use artificial neural networks as our classifiers in the six-class problem. The input features are mainly extracted from pattern spectra of nucleus. To be more specific, we use six features – two are area-based, the remaining four are morphology-based.

1. Mathematical Morphology

Mathematical morphology is a branch of nonlinear image processing and analysis. Morphological methods are used in many ways in image processing, for example, enhancement, segmentation, restoration, edge detection, texture analysis, shape analysis, etc. It is also applied to several research areas, such as, medical imaging, remote sensing, military applications, etc.

2. Morphological Operations

Morphological operations are non-linear, translation invariant transformations. We describe binary morphological operations only. Binary images can be considered as functions on two dimensional grids with values of 0 or 1 or, equivalently, as characteristic functions of subsets of the two-dimensional plane. The concept of structuring element is fundamental in morphology; it is the analogue of a convolution mask in linear image processing. The basic morphological operations involving an image S and a structuring element E are

erosion: $S \ominus E = \bigcap \{S - e : e \in E\}$
dilation: $S \oplus E = \bigcup \{E + s : s \in S\}$,

where \cap and \cup denote the set intersection and union, respectively. $A + x$ denotes the translation of a set A by a point x , i.e.

$$A + x = \{a + x : a \in A\}.$$

The closing and opening operations, derived from the erosion and dilation, are defined by

$$\text{closing: } S \oslash E = (S \oplus (-E)) \ominus (-E)$$

$$\text{opening: } S \circ E = (S \ominus E) \oplus E$$

where $-E = \{-e : e \in E\}$ denotes the 180° rotation of E about the origin.

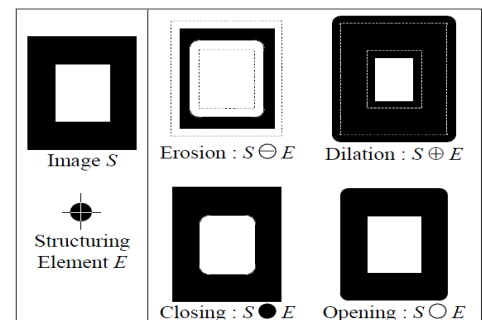


Fig. 2 Samples of an image S , structuring element E , and outputs of the erosion, dilation, closing and opening operators.

3. Pattern Spectrum

We successively apply the opening operation to an image and increase the size of structuring element in order to diminish the image. Let $\Omega(t)$ be area of $S \cap E$ where t is a real number and $\Omega(0)$ is area of S . $\Omega(t)$ is called a *size distribution*. The normalized size distribution $\Phi(t) = 1 - \Omega(t)/\Omega(0)$, and $d\Phi(t)/dt$ are called *granulometric size distribution* or *pattern spectrum* of S .

4. Feature Extraction

We focus our feature extraction on themorphology - based features. Hence, we will introduce their derivations here. For a random set S , $\Omega(t)$ is a random function. The normalized size distribution $\Phi(t) = 1 - \Omega(t)/\Omega(0)$, the so-called *pattern spectrum* of S , is a probability distribution function. Its moments, $\mu(1)(S), \mu(2)(S), \dots$, are therefore random variables namely *granulometric moments*. In this research, we consider nuclei as an object of interest. We calculate a pattern spectrum of each cell's nuclei and calculate the first and second granulometric moments of the pattern spectrum to achieve our features. We also extract two other features from each nucleus, i.e., the area of the nucleus and the location of its pattern spectrum's peak. We, therefore, determine four feature values for each cell image. To form an input feature vector to a neural network, we extract six features from each cell, i.e.,

- o the area of cell,
- o the nuclei-to-cytoplasm ratio,
- o the maximum value of a pattern spectrum,
- o the location where the maximum value of a pattern spectrum occurs,
- o the first granulometric moments and
- o the second granulometric moments.

We select a small digital disc as the structuring element in our experiments. The structuring element is shown in Figure 3.

0	1	1	0
1	1	1	1
1	1	1	1
0	1	1	0

Fig. 3 Structuring element used in the experiments.

5. Bayes Classifier

Bayes classifier is a traditional statistical-based classifier that analyzes discriminant functions by using Bayes' theorem. Consider a classifier, we assign an input vector x to class C_k if $y_k(x) > y_j(x)$ for all $j \neq k$. By choosing $y_k(x) = P(C_k|x)$, this posterior probability is the probability of pattern belonging to class C_k when we observe the input vector x . Bayes' theorem yields $y_k(x) = P(C_k|x) = \frac{p(x|C_k)P(C_k)}{p(x)}$, (9) where $p(x)$ is the unconditional density and $P(C_k)$ is the prior probability of the k th class. Assuming the conditional probability density is normal, i.e.,

$$p(x|C_k) = \frac{1}{(2\pi)^{d/2} |\sum_k|^{1/2}} \exp\left(-\frac{1}{2}(x-\mu_k)^T \sum_k^{-1} (x-\mu_k)\right), \tag{10}$$

$$y_k(x) = P(C_k|x) = \frac{p(x|C_k)P(C_k)}{p(x)},$$

$$\ln(y_k(x)) = -\frac{d}{2}\ln(2\pi) - \frac{1}{2}\ln(|\sum_k|) - \frac{1}{2}(x - \mu_k)^T \sum_k^{-1} (x - \mu_k) + \ln(P(C_k))$$

A theorem describing how the conditional probability of a set of possible causes for a given observed event can be computed from knowledge of the probability of each cause and the conditional probability of the outcome of each cause

$$\text{Posterior} = \frac{\text{likelihood} \times \text{prior}}{\text{normalizing constant}}$$

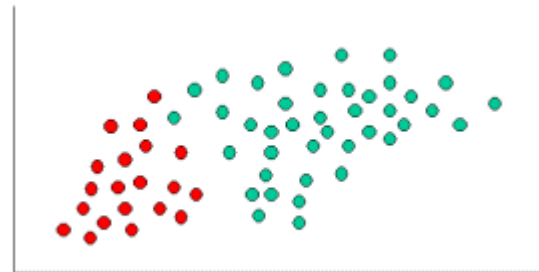


Figure 4. Objects classified as RED and GREEN

Here the objects can be classified as either GREEN or RED. Our task is to classify new cases as they arrive, i.e., decide to which class label they belong, based on the currently existing objects. Since there are twice as many GREEN objects as RED, it is reasonable to believe that a new case (which hasn't been observed yet) is twice as likely to have membership GREEN rather than RED. In the Bayesian analysis, this belief is known as the prior probability. Prior probabilities are based on previous experience, in this case the percentage of GREEN and RED objects, and often used to predict outcomes before they actually happen.

Thus, we can write:

$$\text{Prior probability for GREEN} \propto \frac{\text{Number of GREEN objects}}{\text{Total number of objects}} \tag{1}$$

$$\text{Prior probability for RED} \propto \frac{\text{Number of RED objects}}{\text{Total number of objects}} \tag{2}$$

Since there is a total of 60 objects, 40 of which are GREEN and 20 RED, our prior probabilities for class membership are:

$$\text{Prior probability for GREEN} \propto \frac{40}{60} \tag{3}$$

$$\text{Prior probability for RED} \propto \frac{20}{60} \tag{4}$$

Having formulated our prior probability, we are now ready to classify a new object (WHITE circle). Since the objects are well clustered, it is reasonable to assume that the more GREEN (or RED) objects in the vicinity of X, the more likely that the new cases belong to that particular color. To measure this likelihood, we draw a circle around X which encompasses a number (to be chosen a priori) of points irrespective of their class labels. Then we calculate the number of points in the circle belonging to each class label. From this we calculate the likelihood:

$$\text{Likelihood of X given GREEN} \propto \frac{\text{Number of GREEN in Vicinity of X}}{\text{Total number of GREEN ases}} \tag{5}$$

$$\text{Likelihood of X given RED} \propto \frac{\text{Number of RED in Vicinity of X}}{\text{Total number of RED cases}} \tag{6}$$

6. Morphological Separation

Overlapped and cluttered cells are an inevitable, unsolved, and usually ignored problem in blood slide analysis. It is up to the technician to choose an ideal work area in the smear where the cells are neither too cluttered nor to disperse. In the more disperse area the cells extend due to the lack of pressure and lose characteristic morphology and in the cluttered area they are indistinguishable one from the other. We have proposed automated criteria for the choosing of an ideal area. Our approach has been to use the morphology of the background-cell border as an initial approach to the cells forms, using a priori knowledge of the cell. We later make use of local information, such as edges or greyscale connectivity, in a top down segmentation scheme to refine the classifying and find cells deeper down the cluster. The watershed algorithm has been widely used as it subdivides the image in catchment basins and clusters together pixels based on spatial proximity and similarity of the gradient.

7. Separation of overlapped blood cells

Figure 5 summarizes the process of cell separation once the overlapped region is identified. In order to split the overlapped regions we obtain the edges of the region and its

centroid and we provide some concave points as points of separation. Then we transform edges from a Cartesian to a polar space, and we interpolate discontinuous points using a linear interpolation. This allows completing cell borders with a conical shape. Finally we join some edges discontinuities by applying morphological operations.



Figure 5: Cell Separation Procedure

III. DATA DESCRIPTION

We used the gray-scale bone marrow images. The images were taken from a slide of a patient's bone marrow smear, without any information about his/her health condition, by an Olympus BX50 microscope, a Sony B/W charge-coupled device (CCD) camera, and an 8-bit digitizer (PDI IMAXX.). Magnification of 600x was used without any special filters. Each white blood cell image was cropped manually to form a single-cell image. Then, a single-cell image was segmented manually into nucleus, cytoplasm, and background region. The data set consists of six classes of white blood cells—myeloblast, promyelocyte, myelocyte, metamyelocyte, band, and PMN.

IV. EXPERIMENTAL FRAMEWORK

Four features are extracted from each cell's nucleus. The features are used as the inputs to two types of classifiers, i.e., a Bayes classifier and an artificial neural network classifier. A fivefold cross validation is applied to let us perform the training and testing on the data set. The classification results are evaluated in terms of the traditional classification rate and the classwise classification rate. In this section, we describe the nucleus feature extraction, the classification performance evaluation, and the experimental results and analysis.

1. Classwise Classification Rates

In a classification problem, we generally evaluate a classifier's performance using the traditional classification rate, which is the ratio of the total correct classifications to the total number of samples classified. In addition to the traditional classification rate calculation, we consider another rate called the classwise classification rate. Basically, the classwise classification rate is the average of the classification rates of all classes, i.e.,

$$\text{classwise classification rate} = \frac{1}{C} \sum_{i=1}^C \frac{\text{number of correct classification in class } i}{\text{total number of samples in class } i} \tag{7}$$

Where C is the number of classes. The basic idea of the classwise rate is to take out the effects of the number of samples in the training. While the traditional classification rate may be high if a large number of correct classifications occur in a class consisting of a large number of samples, the classwise rate is high only if all the classes have large numbers of correct classifications compared to their corresponding total number of samples. Therefore, we

prefer to have a classifier that provides good classification performance in both the traditional and class wise senses.

2. Experimental Methods

Both the Bayes classifier and artificial neural network classifier require supervised learning, i.e., training and testing with known classified samples. From the data description, the available data set is not divided into training and test sets; however, we need to have training and test sets to train and test our classifiers to evaluate their generalization properties. We, therefore, apply the cross validation method, which is a standard solution of the aforementioned limitation. The experiments are performed using the fivefold cross validation method.

2.1) Bayes' Classifiers:

We initially performed the cell classification using Bayes classifiers due to their simplicity. It is assumed that the conditional probability density is normal. There are two parts in the experiments of evaluating our features using Bayes' classifiers. First, the *a priori* class probabilities $P(C_k)$ are calculated from the proportion of the numbers of cells in the training set and second, all the six cell classes are assumed

equally likely, i.e., $P(C_k) = 1/6$, $k = 1, 2, \dots, 6$.

2.2) Neural Networks:

We chose a feedforward neural network consisting of one hidden layer of five hidden neurons. The desired output was set to 0.9 for the output neuron corresponding to the labeled class, and 0.1 for the other output neurons. The networks were trained using the LM algorithm. The training stops when the maximum number of epochs reaches 100 or the mean square error is less than 10^{-6} . From the results obtained for the Bayes classifiers, we guessed that the same generalization problem would also happen for neural networks. To cope with the problem, we changed the desired output value such that it was smaller for a class that contains a larger number of samples. We achieved that by setting the desired output of the labeled class to

$$d = 1 - \frac{\text{number of training samples in labeled class}}{\text{total number of training samples}} \quad (8)$$

and setting d equal to zero for all other classes. For each setting of the desired outputs, we performed a fivefold cross validation procedure 50 times in order to analyze the effects of randomness from the sample selection in the cross validation and the neural networks' initializations. Hence, we trained and tested (two settings) \times (fivefolds) $\times 50 = 500$ networks in total.

3. Subsets of the Proposed Nucleus-Based Features:

To analyze the correlation among the proposed features, we performed the classification on all possible combinations of these features. From the four features, we ended up with 15 possible combinations. We denote the area, peak location, and the first and second granulometric moments by f_1 , f_2 , f_3 , and f_4 , respectively. We trained and tested neural network classifiers with fivefold cross validation and the parameters mentioned in Section IV-C2.

4) Comparison to Other Nucleus-Based Features:

To compare our proposed features to other previously proposed nucleus-based features, we trained and tested Bayes classifiers and neural networks with fivefold cross validation on our defined data set.

5. Comparison to Other Classifiers:

We further investigated the use of our proposed nucleus-based features on two other classifiers—the naive Bayes classifier and the C4.5 decision tree—with fivefold cross validation. These classifiers were implemented using the Waikato Environment for Knowledge Analysis (WEKA), which is a collection of machine learning Algorithms.

TABLE I. CLASSIFICATION RESULTS OF BAYES CLASSIFIERS

Training Bias	Classification rate			
	Traditional		Class-wise	
	Train	Test	Train	Test
P(C _k) is in proportion to No. of training samples	81.15	77.49	73.25	63.39
P(C _k)=1/6	73.90	69.37	82.17	68.08

TABLE II. CLASSIFICATION RESULTS OF NEURAL NETWORKS

Desired output setting	Classification rate(mean+standard deviation)			
	Traditional		Class-wise	
	Train	Test	Train	Test
d=0.9 for the labeled class	80.63±	77.05±	59.34±	54.80±
d=0.1 for others	0.36	0.87	1.17	0.92
d is as in (3) for the labeled class	73.90	69.37	82.17	68.08
d=0.1 for others	0.72	1.15	2.17	2.02

V. RESULTS AND ANALYSIS

1. Results for Bayes' Classifiers

Table I shows the classifier's performance. When *a priori* class probabilities are calculated from the numbers of cells in the training sets, we can see that the traditional classification rates of the classifiers on the training and test sets are 81% and 77%, respectively, and for the classwise classification, 73% and 63%, respectively. Most of the training and test cells are classified as myelocyte or PMN. This is because the *a priori* probabilities of these two classes are much larger than the others. On the other hand, the classwise classification rates are not that high. It should be noted that, in practice, the *a priori* probabilities of cell occurrences are not known in advance. Therefore, using Bayes classifiers with *a priori* probabilities in proportion to the numbers of training cells may not be a feasible approach. When we make the classification "fair" by setting the *a priori* probabilities of all the six classes to 1/6, there are less correct classifications in the two big classes, but more correct classifications in the classes with small numbers of samples. In this case, even though the traditional classification rates drop in the training and test sets, the classwise classification rates increase. In a real-

world situation, it makes sense to use the classwise classification measure because it gives equal importance to each cell class, and we do not usually know the exact proportion of cell classes in advance.

2. Results for Neural Networks

The average classification rates are shown in Table II. The networks trained regularly achieved the traditional classification rates of 81% and 77% on the training and test sets, respectively. However, the classwise classification rates were very low at 59% and 55%, respectively.

TABLE III. CLASSIFICATION RESULTS OF SUBSETS OF THE PROPOSED FEATURE

Feature Subset{FS}	classification rate(%) {CR}	{FS}	{CR}	{FS}	{CR}
{f1}	53.60	{f1,f3}	75.41	{f1,f2,f3}	73.55
{f2}	71.46	{f1,f4}	74.48	{f1,f2,f4}	73.09
{f3}	73.32	{f2,f3}	73.55	{f1,f3,f4}	75.41
{f4}	73.29	{f2,f4}	72.39	{f2,f3,f4}	74.48
{f1,f2}	74.01	{f3,f4}	73.32	{f1,f2,f3,f4}	76.8

The networks trained by setting the desired outputs as in (2) accomplished similar performance to that with the first setting when evaluated by the traditional classification rate, i.e., 83% and 77% on the training and test sets, respectively. However, it yielded the better classwise classification rates of 74% and 61%, respectively. The numbers of correct classifications of the classifiers trained using two different desired output settings in the big classes are similar. However, the classifiers trained using the desired outputs as in yielded much better classification in the small classes such as promyelocyte and metamyelocyte. As a result, similar classification performances were achieved by the two settings in the traditional sense, but the setting as in yielded much better performance in the classwise sense. Similar results occurred in the testing. There were more correct classifications in the small classes. The traditional classification rates of both settings were similar. However, the classifiers trained with the desired output set as in (2) yielded the better classwise classification rate compared to that achieved by the classifiers trained regularly. For both classifiers, most misclassified cells are in adjacent classes. This is not surprising because of similarities between adjacent classes. An expert would also have to classify each of them to a class or its corresponding adjacent class. One more observation from our experiments is that the classifiers are biased toward the classes with larger numbers of training samples, which is a way to achieve high traditional classification rate. The classwise classification rate provides more information in this case. Our results suggest that the classwise classification rate increases when we suppress the bias by the numbers of training samples. In Bayes classifiers, when the bias suppression is applied, the classwise classification rates increase, but unfortunately, the traditional classification rates drop. More interesting results can be seen in the experiments using neural networks. The bias suppression using (2) does not decrease the traditional classification rates. However, it does increase the classwise classification

rates. Therefore, the neural network classifier using the bias suppression of (2) is the favorite choice because it yielded better classification performances in both traditional and classwise senses.

3. Analysis of the Subsets of the Proposed Nucleus-Based Features

The traditional classification rates on the test sets using each combination of these features are shown in Table III. We can see that the highest classification rate is achieved when all four features are employed as expected

TABLE IV. CLASSIFICATION RESULTS USING NUCLEUS-BASED FEATURES

Classifier	Training Bias	Classification rate(%)			
		Traditional		Class-wise	
		Train	Test	Train	Test
Bayes	P(Ck) is in proportion to No. of training samples	81.15	77.49	73.25	63.39
	P(Ck)=1/6	73.90	69.37	82.17	68.08
Neural Network	d=0.9 for the labelled class d=0.1 for others	80.63± 0.36	77.05± 0.87	59.34± 1.17	54.80± 0.92
	d is as in (3) for the labeled class d=0.1 for others	73.90 0.72	69.37 1.15	82.17 2.17	68.08 2.02

4. Results for the Comparison to other Nucleus-Based Features

The classification rates are shown in Table IV that summarizes the overall results. Comparing classification results in Table IV to those in Tables I and II, we can see that our nucleus-based features yield better classification performances when using the Bayes classifier. For the neural network case, even though the performances on the training sets are similar, the rates achieved by using our proposed nucleus-based features are higher than those achieved by the other features proposed previously.

CONCLUSION

We analyzed the white blood cell classification using only features extracted from the image of the nucleus. Specifically, the six-class classification problem of white blood cells in myelocytic series was considered. We performed the experiments on the white blood cell images taken from different areas in one slide. Features based on the morphological granulometries were extracted from each manually segmented blood cell's nucleus. It should be noted that manual segmentation was performed only in this investigation step. In a real automatic system, the nucleus segmentation will be performed automatically. From our experiments, it was shown that using only the nucleus-

based features produced promising results. In addition to the traditional classification rate, we considered the classwise classification rate, where the classification rate of each class is calculated separately and averaged over all classes at the end. Consider the Bayes classifiers trained by calculating the *a priori* class probabilities from the proportion of the numbers of cells in the training set, they may not be feasible because the number of cells in each class is not practically known in advance. From our results, the Bayes and the neural network classifiers are biased toward the classes with large numbers of training samples. The classwise classification rate is improved when all classes are assumed equally likely. Extensive experiments were performed on neural networks. We initially trained neural networks by setting the desired output to 0.9 for the labeled class and 0.1 for the other classes. Good traditional classification rates were achieved. Meanwhile, the classwise classification in rates were low. To suppress the effects of the number of training samples in a class, we set the desired output for the labeled class and 0 for the other classes. With that setting, good traditional and classwise classification rates were accomplished. In practice, the neural networks trained with bias suppression will be selected because they yield good classification rates in both traditional and classwise senses. We analyzed feature subsets to show that all the four proposed features are important. We also compared the classification performances based on our proposed features to those of other previously proposed nucleus-based features using the same cell data set. The results showed that classifiers using our proposed features yielded better classification performances. Classification using the naive Bayes classifier and the C4.5 decision tree were also performed using our proposed features. The classification performances of these two classifiers were shown to be not as good as those of the Bayes classifiers and neural network classifiers. It was seen that most of the misclassifications occurred in adjacent classes. These misclassified cells may be those which give feature vectors close to the decision boundary between the adjacent classes. This classification disagreement for cells at the boundary also occurs in expert classification. We have shown that the application of only nucleus-based features to the problem of automatic bone marrow white blood cell classification is very promising. Segmentation in an automatic cell classification system can be down-scaled to just segmenting nuclei, which is much easier than the segmentation of both the nucleus and cytoplasm.

References

- [1] Bennett, J.M., Catovsky, D., and Daniel, M.T., *Proposals for the classification of the acute leukaemias*. British Journal of Haematology, 1976. **33**(4): p. 451-458.
- [2] Park, J. and Keller, J.M., *Snakes on the watershed*. IEEE Transactions On Pattern Analysis And Machine Intelligence, 2001. **23**(10): p. 1201-1205.
- [3] Keller, J.M., Gader, P.D., et al. *Soft counting networks for bone marrow differentials*. 2001: Systems, Man, and Cybernetics, 2001 IEEE International Conference on.

[4] Jae-Sang, P. and Keller, J.M. *Fuzzy patch label relaxation in bone marrow cell segmentation*. in *Systems, Man, and Cybernetics*. 1997: IEEE International Conference on.

[5] Sobrevilla, P., Montseny, E., and Keller, J., *White blood cell detection in bone marrow images*, in *18th International Conference of the North American Fuzzy Information Processing Society - Nafips*, R.N. Dave and T. Sudkamp, Editors. 1999, I E E E: New York. p. 403-407.

[6] Theera-Umpon, N., *White blood cell segmentation and classification in microscopic bone marrow images*, in *Fuzzy Systems And Knowledge Discovery, Pt 2, Proceedings*. 2005, Springer-Verlag Berlin: Berlin. p. 787-796.

[7] Nilsson, B. and Heyden, A., *Segmentation of complex cell clusters in microscopic images: Application to bone marrow samples*. Cytometry Part A, 2005. **66A**(1): p. 24-31.

[8] Zhang, X.W., Song, J.Q., et al., *Extraction of karyocytes and their components from microscopic bone marrow images based on regional color features*. Pattern Recognition, 2004. **37**(2): p. 351-361.

[9] Montseny, E., Sobrevilla, P., and Romani, S., *A fuzzy approach to white blood cells segmentation in color bone marrow images*, in *2004 IEEE International Conference on Fuzzy Systems, Vols 1-3, Proceedings*. 2004, IEEE: New York. p. 173-178.

[10] Meschino, G.J. and Moler, E., *Semiautomated image segmentation of bone marrow biopsies by texture features and mathematical morphology*. Analytical And Quantitative Cytology And Histology, 2004. **26**(1): p. 31-38.

[11] Hengen, H., Spoor, S., and Pandit, M. *Analysis of blood and bone marrow smears using digital image processing techniques*. 2002. San Diego, CA, United States: The International Society for Optical Engineering.

[12] <http://www.cri-inc.com>.